Can Eddy Fluxes Serve as a Catalyst for Hurricane and Typhoon Formation?*

MALAKONDAYYA CHALLA

Geophysical Fluid Dynamics Institute, The Florida State University, Tallahassee, Florida

RICHARD L. PFEFFER

Geophysical Fluid Dynamics Institute and Department of Meteorology, The Florida State University, Tallahassee, Florida

QIANG ZHAO

Geophysical Fluid Dynamics Institute, The Florida State University, Tallahassee, Florida

SIMON W. CHANG

Naval Research Laboratory, Monterey, California

(Manuscript received 21 February 1997, in final form 25 September 1997)

ABSTRACT

Numerical simulations and diagnostics are performed for Typhoon Tip and Tropical Storm Faye, both of which occurred during 1979, the year of the First Global GARP (Global Atmosphere Research Program) Experiment (FGGE). The simulations are started from early in the life cycles of both disturbances, the former of which developed into a super typhoon, and the latter of which did not develop beyond the tropical storm stage. The numerical model employed was that of Madala et al. and is a modification of the one used in previous simulations by the authors. The primary modifications are the inclusion of a more sophisticated boundary layer parameterization, based on similarity theory, and the inclusion in the Kuo cumulus parameterization scheme of the nonmeasurable mesoscale latent heat release, as described by Krishnamurti et al. The initial conditions for both simulations were derived from the FGGE dataset of the European Centre for Medium-Range Weather Forecasts and from monthly mean sea surface temperatures provided by the National Meteorological Center (now the National Centers for Environmental Prediction). The initial intensities and the underlying sea surface temperatures were approximately the same for the two disturbances. In the simulations, Tip developed into an intense typhoon and Faye did not develop, as observed in the atmosphere, although the minimum surface pressures and maximum wind speeds attained do not agree quantitatively with the reported values.

The primary question the authors set out to answer is what special conditions exist at the early stages of the life cycles of tropical disturbances that allow one system to develop and another to fail to develop into a typhoon. The most significant difference found in the initial states of Tip and Faye was a large-scale eddy flux of angular momentum from the surroundings into the former and out of the latter, with maximum amplitudes located around 200 mb at radial distances from the vortex centers greater than 1000 km. These fluxes persisted for at least 24 h prior to the time the numerical simulations were started. While there were differences in the eddy heat fluxes as well, these were less significant. Diagnostic calculations reveal that the secondary radial circulation induced by the eddy fluxes of momentum and heat transported water vapor inward for Tip and outward for Faye, with the result that convection broke out at an early stage in the vortex center of Tip, but not in Faye. The convection intensified with time in Tip and subsequently became the dominant factor contributing to the moisture inflow and rapid vortex intensification.

The authors' interpretation of the results of their numerical simulations and diagnostic calculations is that the secondary radial circulation induced by large-scale eddy fluxes of heat and momentum can serve either as a catalyst for typhoon formation or as a mechanism for inhibiting the further development of an incipient tropical disturbance, depending on the direction of the water vapor transport (into or out of the vortex core).

1. Introduction

Hurricanes and typhoons are rare events in nature when compared to the large number of cloud clusters and depressions that cross sufficiently warm ocean waters every summer season. This suggests that external conditions in the background field in which tropical disturbances form and travel must play a role in enhancing or suppressing their development. Meteorologists have long sought to determine what these special conditions are and how they operate.

Ooyama (1964) and Charney and Eliassen (1964) suggested that tropical disturbances intensify through a cooperative arrangement between deep cumulus clouds and a large-scale vortex, such that the Ekman circulation induced by the vortex concentrates the moisture required

* Geophysical Fluid Dynamics Institute Contribution Number 385.

Corresponding author address: Prof. Richard L. Pfeffer, Geophysical Fluid Dynamics Institute, The Florida State University, Tallahassee, FL 32306-4360.
E-mail: pfeffer@gfdi.fsu.edu

by the cumulus convection, while the latent heat released by the convection drives the radial circulation. Through the action of the Coriolis force, the radial circulation intensifies the vortex, which, in turn, intensifies the frictional inflow, thereby bringing more moisture into the region, setting off more convection and further intensifying the vortex. The Ekman circulation in this scenario plays the dual role of providing the water vapor and the upward motion to set off conditional instability in the tropical atmosphere.

Emanuel (1986, 1989) has argued that the degree of conditional instability in the Tropics is just enough to sustain convection against dissipation due to entrainment, so that effectively there is no preexisting convective available potential energy (CAPE) for the formation of hurricanes. He suggests that hurricane development takes place as a result of finite amplitude instability involving feedback between an incipient tropical cyclone and wind-induced evaporation in the absence of significant CAPE. Emanuel's concept is that the strong surface winds associated with a sufficiently intense vortex over sufficiently warm water will enhance evaporation from the sea in the inner core of the vortex. Cumulus convection renders the lapse rate nearly neutral to slantwise convection along constant angular momentum surfaces. This convection takes place at progressively higher equivalent potential temperatures as the excess evaporation continues. The cumulus mass flux associated with the deep cumulus clouds drives a radial circulation that, through the action of the Coriolis force, intensifies the vortex.

Both conditional instability of the second kind (CISK) and the finite amplitude air–sea interaction mechanism can operate in purely symmetric vortices. Both require a threshold intensity of the initial symmetric vortex that is greater than what we find in nature during the early cloud cluster and depression stages of tropical storm development. An important question to be addressed then is, what are the processes that enhance the development of a small number of tropical cloud clusters and depressions in nature to the point that they can reach the threshold intensity required for self-sustained growth to hurricane intensity?

In a series of investigations, the present writers (Challa and Pfeffer 1980, 1984, 1990, 1992; Pfeffer and Challa 1981, 1982, 1992, 1993) have explored the possible role of inward eddy fluxes of angular momentum and heat in the initial organization and spinup of tropical disturbances. Our work has been motivated by the observational studies of Pfeffer (1956, 1958, 1965), Palmen and Riehl (1957), Black and Anthes (1971), and Frank (1977) that revealed the presence of significant large-scale eddy fluxes of momentum into hurricanes, and by the theoretical work of Eliassen (1952) and Kuo (1956) that demonstrated how eddy fluxes of momentum and heat induce secondary circulations. In the context of hurricane formation, such secondary circulations, when directed inward into a lower tropospheric vortex over a broad stretch of warm tropical ocean, can concentrate moisture and stimulate deep cumulus convection in the core of the incipient disturbance. The latent heat release associated with this organized convection causes vortex stretching in the lower troposphere that intensifies the low-level vortex. An alternative view of the role of upper-level forcing in hurricane formation has been presented by Montgomery and Farrel (1993) from the perspective of PV (potential vorticity) thinking. From this perspective, upper-level momentum fluxes into the region occupied by a low-level tropical vortex create an upper-level PV anomaly that, in a nearly neutrally stable moist environment, induces rising motion in a deep layer over the vortex and, through vortex stretching, intensifies the low-level system. Additional support for the hypothesis that eddy fluxes play an important role in hurricane dynamics comes from a study by Davidson et al. (1990), who presented evidence to the effect that upper-level eddy fluxes of momentum were important in the genesis of Tropical Cyclones Irma and Jason in the Australian region. Studies by Molinari and Vollaro (1989, 1990), DeMaria et al. (1993), and Shi et al. (1997) have also provided evidence of the importance of upper-level eddy fluxes of momentum in the reintensification of hurricanes during their life cycles.

Our past efforts to study the role of synoptic-scale eddy forcing have involved the use of different numerical models to simulate the evolution of initial disturbances defined by the Colorado State University composite dataset (McBride 1981a,b; McBride and Zehr 1981). These disturbances include Atlantic cloud clusters and depressions that developed into hurricanes and ones that did not. A significant difference seen in the Colorado State datasets between the initial states for the developing and nondeveloping disturbances is the presence in the former, and absence in the latter, of a well-organized inward eddy flux of angular momentum in the upper troposphere at radii greater than 500 km.

In our early work we used Sundquist's (1970) symmetric hurricane model in which we parameterized the eddy fluxes of momentum. In our numerical simulations with this model, hurricanes developed from initial conditions corresponding to the composite data for developing disturbances and did not develop from initial conditions corresponding to the data for nondeveloping disturbances. Calculations of the energetics in the developing cases revealed that the eddy fluxes played the dominant role in the earliest stages of vortex intensification. The subsequent explosive growth was associated with work done by the symmetric flow across the isobars.

In our later investigations we used the 3D Naval Research Laboratory (NRL) mesoscale model developed by Madala and Chang (1979) and Madala et al. (1987), which is a version of the Navy Operational Regional Atmospheric Prediction System (NORAPS). As in the earlier simulations with Sundquist's model, hurricanes

developed from the initial conditions corresponding to the developing disturbances and did not develop from those corresponding to the nondeveloping disturbances. To test further the importance of eddy fluxes as a catalyst for hurricane genesis we also ran numerical experiments in which these fluxes were omitted from the initial conditions for the developing disturbances by using only the symmetric components of the initial wind and temperature fields corresponding to these disturbances. In these model integrations such initial vortices did not develop.

As a diagnostic tool we solved the Eliassen–Kuo meridional circulation equation using the model output from the integrations with both the symmetric and full initial conditions for developing tropical disturbances to determine the roles of the different forcing functions (diabatic heating, friction, and eddy fluxes of momentum and heat). Since this equation is linear, the complete solution was obtained as the sum of the solutions induced by the separate forcing functions. These solutions revealed that the effect of the eddy fluxes of heat and momentum was to drive a weak but persistent radial circulation during the early stages of vortex intensification with broad-scale inflow in the lower troposphere, upward motion near the axis of the vortex, and outward motion in the vicinity of the tropopause. In the absence of these fluxes the components of the radial circulation driven by diabatic heating and friction were much weaker than in their presence. Our interpretation of this result is that the eddy-flux-driven radial circulation organizes the convection that is present in the region and picks up additional water vapor from the warm ocean at large radii, which it concentrates in the inner vortex region. This triggers additional deep cumulus convection and enhanced heating in the center of the vortex. The heating intensifies the radial circulation and, through the agency of the Coriolis force, the vortex intensifies. The more intense vortex generates more vigorous local evaporation and Ekman pumping, which further increases the equivalent potential temperature in the planetary boundary layer. This sequence of events is responsible for the development of the disturbance to a threshold intensity, beyond which explosive growth by either the CISK or air–sea interaction mechanism becomes possible. In the absence of the eddy fluxes, the primary mechanism available to concentrate the moisture and initiate deep cumulus convection is Ekman suction, as postulated by Ooyama (1964) and Charney and Eliassen (1964). In the early stages of development of cloud clusters and depressions, however, the initial vortex is not strong enough to provide a sufficiently intense Ekman circulation to set off the deep cumulus convection required for self-sustained growth to hurricane intensity. Moreover, it is not strong enough to provide the moisture required through local evaporation for the air–sea interaction mechanism of Emanuel to initiate the process of intensification.

The evidence from our numerical simulations with initial conditions derived from composite data seemed sufficiently compelling to suggest that we try using initial data for individual developing and nondeveloping tropical disturbances to explore further the hypothesis that eddy fluxes of heat and momentum can serve as a catalyst in hurricane and typhoon formation. The present paper represents a first step in that direction. In particular, we present the results of two numerical simulations with the NRL mesoscale model with initial conditions derived from ECMWF FGGE IIIb data, specifically, the data at 1200 UTC 7 October 1979 for the tropical depression that later became Supertyphoon Tip and at 0000 UTC 3 July 1979 for the nondeveloping Tropical Depression Faye. At these times the Joint Typhoon Warning Center characterized Tip as a tropical storm and Faye as about to become a tropical storm. It should be noted, however, that the maximum wind speeds in the FGGE dataset on the 1.875° × 1.875° ECMWF grid for these times were 16 and 15 m s^{-1}, respectively, which categorize them as tropical depressions at the beginning of the numerical simulations. Moreover, the maximum azimuthally averaged azimuthal wind speeds were 10 and 9 m s^{-1} at about 875 mb in these disturbances, respectively.

In the following section we summarize the numerical model used in the simulations and we describe the procedure for initialization of the data. Section 3 reviews the history of the two disturbances and compares their structures at the initial times that we chose for our simulations. In section 4 we present the results of the two integrations and in section 5 we show the diagnostics and discuss the mechanisms involved. Our conclusions are presented in section 6.

2. Numerical model, data source, and initialization

The numerical model employed for the present simulations (Madala et al. 1987) is a modification of the one used in our previous simulations (Challa and Pfeffer 1990). The primary modification is the inclusion of a more sophisticated boundary layer parameterization. This model has been used also in simulations by Chang and Holt (1994) and Chang et al. (1996). Briefly, it consists of five prognostic and two diagnostic equations in σ coordinates for the seven dependent variables (viz., eastward and northward velocity components u and v, temperature T, specific humidity q, surface pressure p_s, geopotential ϕ, and vertical velocity $\dot{\sigma}$). The model has 170 × 170 horizontal grid points covering a domain of about 45° lat × 45° long with a grid spacing of 0.27 lat × 0.27 long, respectively. In the vertical it has 16 sigma levels, 7 of which are in the planetary boundary layer with vertical resolution decreasing with height. The lowest layer of the model has a thickness of approximately 50 m. Second-order accurate finite differencing on an Arakawa C grid, which conserves quadratic invariants, was used for the horizontal discretization, and a vertical mode split-explicit leapfrog

scheme, described by Madala (1981), was used for the time integration.

The parameterization of the planetary boundary layer was based on similarity theory (Monin and Yaglom 1971; Businger et al. 1971). The similarity formulation was used to calculate surface fluxes of momentum, sensible, and latent heat in the surface layer. Above the surface layer the turbulent mixing was modeled by a turbulent kinetic energy (TKE) equation and an equation for the rate of dissipation (ϵ) with one and a half order closure. The eddy viscosity k_m in the turbulent mixed layer was expressed, as per Kolmogorov (1942) and Monin and Yaglom (1971), in terms of the turbulent kinetic energy E and the dissipation rate ϵ as

$$k_m = c_1 E^2/\epsilon,$$

where $c_1 = 0.026$. A more complete description of the boundary layer formulation may be found in Gerber et al. (1989) and Holt et al. (1990).

The model physics includes dry convective adjustment, latent heat release in convective and nonconvective clouds, and internal diffusion. Latent heat release and precipitation by convective clouds are parameterized using Kuo's (1974) modified scheme, with the addition of nonmeasurable mesoscale moisture as prescribed by Krishnamurti et al. (1983). Nonconvective latent heat release takes place in the model when convective precipitation is not occurring and when saturation is reached on the resolvable scale. Dry convective adjustment, giving a slightly stable lapse rate without changing the total static energy, is activated when the static energy of a layer exceeds that of the layer just above it.

ECMWF FGGE IIIb data on a 1.875° lat × 1.875° long grid served as the data source for our simulations. A cubic polynomial interpolation scheme was used to interpolate the meteorological variables to the model grid of 0.27° lat × 0.27° long covering a 45° lat × 45° long region. A similar interpolation scheme was used for vertical interpolation from the 15 pressure levels of the FGGE data to the 16 levels in our model. Sponge layers were imposed on the lateral boundaries of the domain and the boundaries were updated with ECMWF data. Following Sashegyi and Madala (1993), we applied the nonlinear normal mode initialization scheme of Bourke and McGregor (1983) to filter the high-frequency gravity waves. This iterative scheme ensures that the amplitudes of the high-frequency gravity waves remain small throughout the numerical integration by requiring that the time tendencies of the divergence and the ageostrophic vorticity be initially zero and that the linearized potential vorticity of the first few vertical modes of the numerical model does not change.

3. Selection of storms

It was our purpose to study the differences between two tropical disturbances with comparable initial intensities, one of which developed into a typhoon and one that did not. Upon examination of the data for the typhoon season of 1979 we selected for the present study the tropical disturbance at 1200 UTC on 7 October that later developed into Supertyphoon Tip and the tropical disturbance at 0000 UTC on 3 July that became Tropical Storm Faye, the intensities of which were nearly the same. At these times the Joint Typhoon Warning Center (JTWC) characterized Tip as a tropical storm and Faye as about to become a tropical storm. Since the atmospheric conditions in Faye met the criteria generally considered favorable for typhoon formation, the JTWC predicted that it would develop into a typhoon, but it did not.

In Figs. 1a–c we compare the initialized surface pressure distribution, wind distribution at $\sigma = 0.86$, and azimuthal mean tangential velocity distribution in the radial plane (with radius defined from the center of lowest pressure) for the two disturbances at the times selected for the initial conditions. The minimum central pressures and maximum wind speeds are 1007.8 and 16 m s^{-1} for Tip and 1009.1 mb and 15 m s^{-1} for Faye. The azimuthal mean tangential wind distributions in Fig. 1c exhibit cyclonic circulations in both storms extending to about 300 mb with the maximum speed of 10 and 9 m s^{-1} for Tip and Faye, respectively. The anticyclonic circulation above 300 mb has a maximum of 2 m s^{-1} and extends to about 700 km in Tip. Faye, on the other hand, exhibits a more well-developed anticyclonic circulation extending to the limits of the data at 1250 km and reaching 7 m s^{-1}. Based on the magnitude of the wind and pressure distributions shown in these figures (which are necessarily smaller than the magnitudes in nature because the data available from the FGGE dataset come from ECMWF model analyses on a comparatively coarse grid, and also because of our initialization) these storms would be classified initially as tropical depressions.

The sea surface temperatures (SST) for both cases were obtained from the National Meteorological Center (now the National Centers for Environmental Prediction) monthly mean sea surface temperature in situ analysis. For Faye we prescribed the June–July mean and for Tip the September–October mean SST distribution. Figure 2 shows the distribution of SST over the domain of integration for Tip and Faye. The SST in the region in which the two disturbances are initially located is above 29°C.

4. Numerical integrations

Starting with the aforementioned initial conditions, we integrated the 3D limited area model for 120 h for Tip and 72 h for Faye. The time variations of the minimum surface pressure and maximum wind at $\sigma = 0.86$, and the observed and predicted tracks for both simulations are shown in Figs. 3a, 3b, and 4, respectively. Tip clearly developed to storm strength by 18 h and to

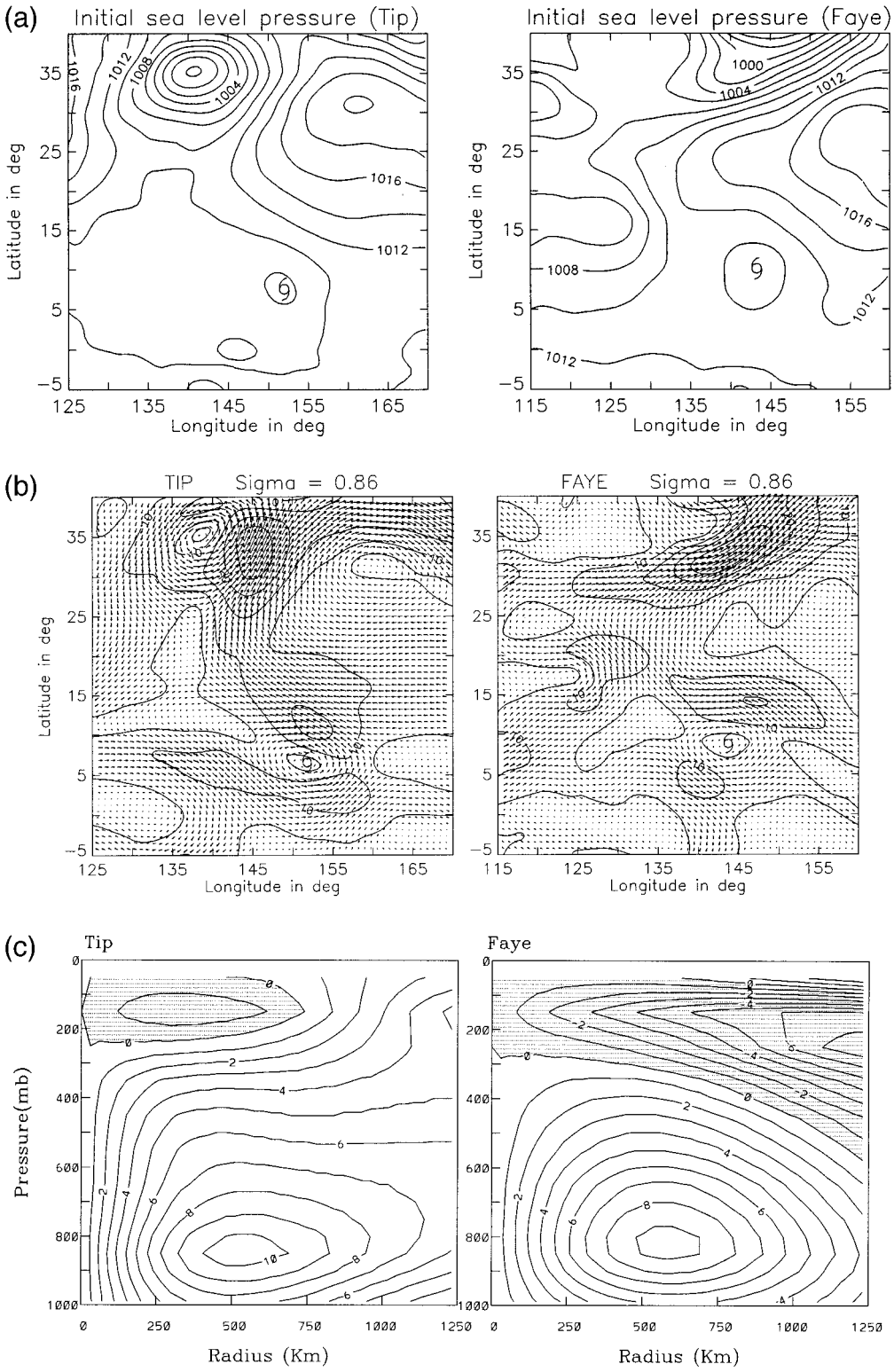

FIG. 1. Initialized data for Tip at 1200 UTC 7 October 1979 (left) and Faye at 0000 UTC 3 July 1979 (right) (a) surface pressure (mb), (b) wind vectors and isotachs (m s^{-1}) at $\sigma = 0.86$, (c) radial cross sections of azimuthal mean tangential velocity (m s^{-1}). Shading represents anticyclonic circulation.

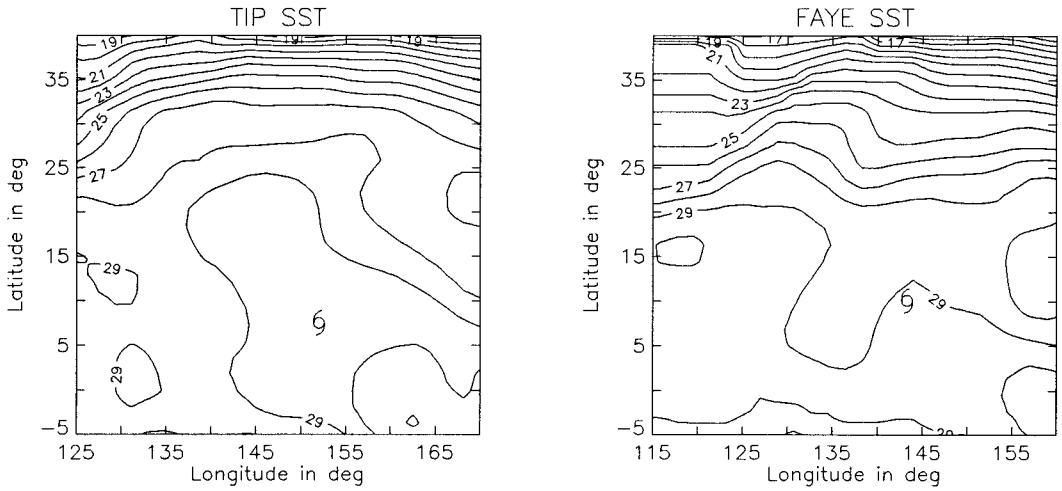

FIG. 2. The mean sea surface temperature distribution for Tip (left) and Faye (right). The SST data is interpolated over land area. Contour interval is 1°C.

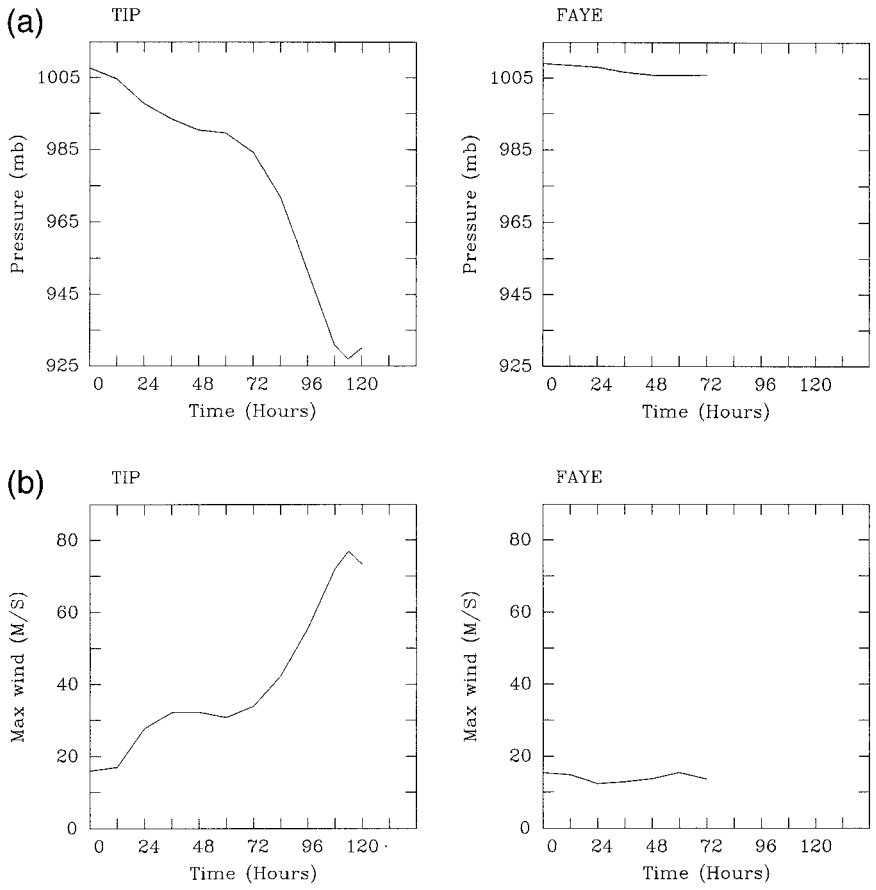

FIG. 3. (a) Time variations of minimum surface pressure for the numerical simulations of Tip (left) and Faye (right). (b) Time variations of maximum wind speed at $\sigma = 0.86$ for the numerical simulations of Tip (left) and Faye (right).

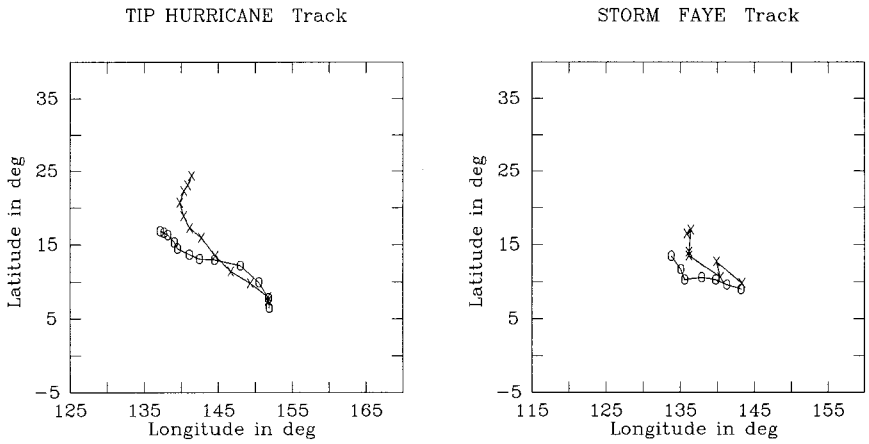

FIG. 4. Predicted (x) and observed (o) tracks of Tip (left) and Faye (right).

hurricane strength by 72 h, subsequently becoming a supertyphoon, whereas Faye did not develop significantly in the simulation, as was the case in nature. The maximum wind of 76 m s^{-1} at 114 h in Tip may be compared with the estimated maximum wind of 85 m s^{-1} by the JTWC about the same time. The minimum surface pressure of 927 mb in our simulation, occurring at the same time as the maximum wind, while very low was not nearly as low as the reported value of 870 mb for Tip. Our predicted track for Tip (Fig. 4) was close to the observed track for the first two days, after which it veered to the north and exhibited recurvature. This northward displacement is similar to the result obtained by Dell'osso and Bengtsson (1985). For Faye, the predicted track was also displaced to the north of the observed track.

A sequence of charts showing the predicted 24-h rainfall rates for Tip is given in Fig. 5. During the first 3 days, when Tip was developing slowly, the maximum rainfall rate increased from 119 to 172 mm d^{-1} and the pattern was consistent with the formation of a spiral band structure and the existence of an active monsoon trough extending from the Marshall Islands through the Caroline Islands to Luzon. As the storm intensified, the maximum rainfall rate increased to 443 mm d^{-1} on the fourth day and to 526 mm d^{-1} on the fifth day, when it reached its maximum intensity. While no data are available concerning the actual rainfall rates in Tip, the maximum value is greater than the amount in a typical hurricane or typhoon (Frank 1977) and is consistent with the status of Tip as a supertyphoon. Moreover, the pattern is similar to that obtained by Dell'osso and Bengtsson, who showed that their precipitation pattern compared favorably with a composite *TIROS-N* visible satellite picture for the 2-h period 1719–1912 UTC 11 October.

The sea level pressure distribution associated with Tip at 114 h and with Faye at 72 h, and the vertical velocity distribution at $\sigma = 0.74$ for both cases are shown in Figs. 6a and 6b, respectively. The vertical velocity field for Tip clearly shows the characteristic spiral band structure of a typhoon and that for Faye is characteristic of a depression.

5. Anatomy of the catalyst

In Figs. 7a,b we show the spatial variations of the latent heat release in the model simulations of Tip and Faye, respectively, at the end of the first time step, and at 30 min and 12, 24, 36, 48, and 60 h. We use the first time step to represent time zero because the latent heat release corresponding to the initialized data is zero. In each of the figures, we have identified the center of the vortex (which is the same as the surface low pressure center) by drawing a broken circle of radius 300 km centered at this location. In both disturbances, the vortex center does not coincide initially with any of the areas of latent heat release. At the end of 30 min of integration, an area of latent heat release breaks out over the vortex center in Tip, but not in Faye. From 12 to 60 h, the vortex center and latent heat release coincide in Tip, whereas the latent heat release pattern in Faye is organized into smaller-scale bands with maximum values far from the vortex center.

In the modified Kuo cumulus parameterization employed in the present simulations, latent heat release takes place only where there is net moisture convergence in a vertical column and mass convergence in the planetary boundary layer. The patterns in Figs. 7a,b suggest that these conditions developed in the center of the vortex early in the simulation of Tip but not in that of Faye. We investigate this situation by calculating the flux of specific humidity across concentric circles centered on the surface low. The curves in Fig. 8 for Tip and Faye, respectively, are based on calculations at radii 30, 60, 90, and 120 km after 30 min of integration in each simulation. The inward moisture flux consists of an axisymmetric component, proportional at each elevation to $\overline{v_r}\,\overline{q}$, and an eddy component proportional to $\overline{v_r'\,q'}$. Here the overbar represents an azimuthal mean and the

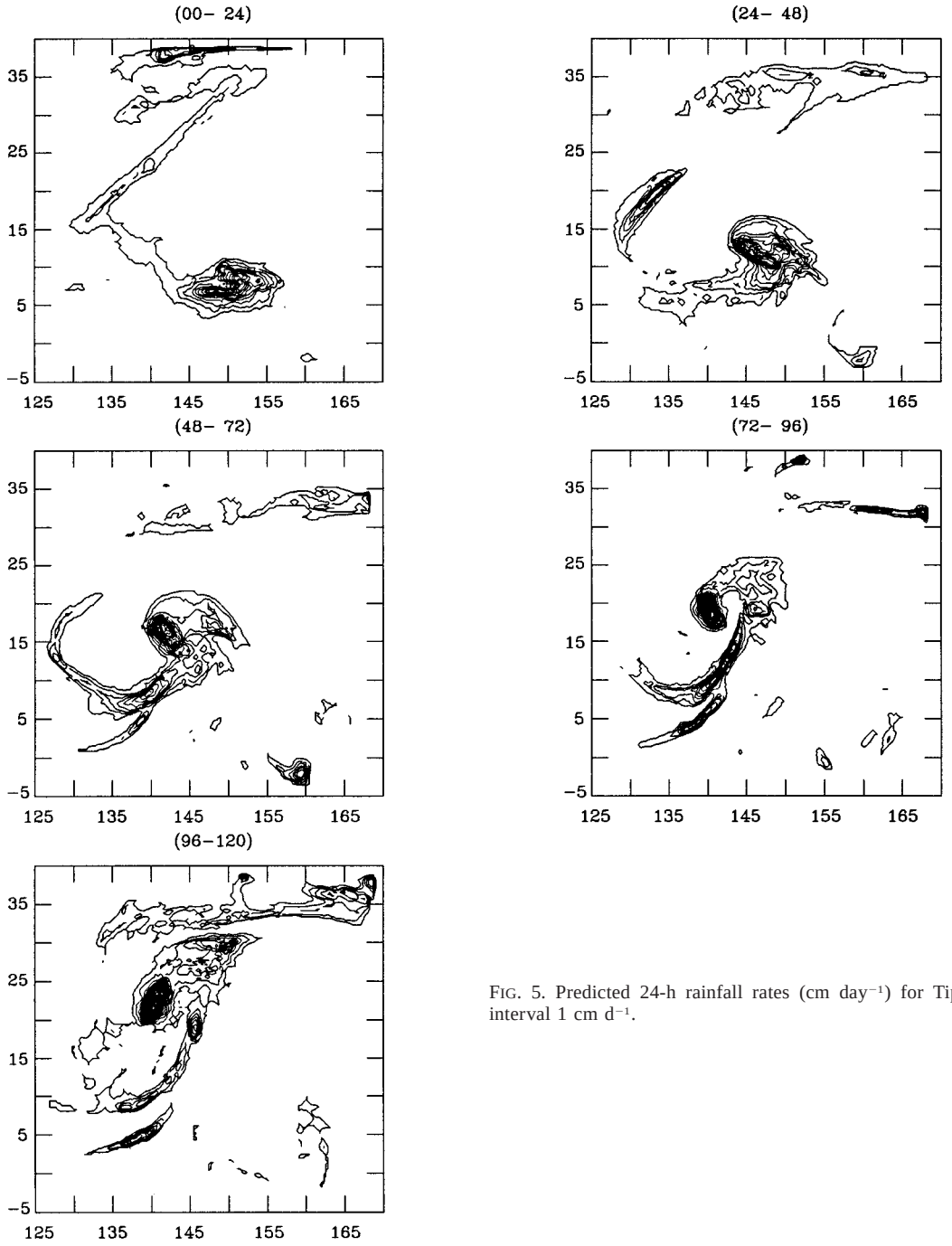

FIG. 5. Predicted 24-h rainfall rates (cm day^{-1}) for Tip. Contour interval 1 cm d^{-1}.

prime a departure from this mean. It is seen that the axisymmetric component is positive in Tip and negative in Faye, whereas the eddy component is slightly negative in Tip and strongly negative in Faye. The net result is that, at this early stage in the simulation, there is a net inward flux of specific humidity into the inner core of Tip, accomplished primarily by the axisymmetric component of the flow, and a net outward flux in Faye, accomplished primarily by the eddy departures from axial symmetry. If we assume that the initial vortices shown in Fig. 1c are balanced vortices, we can use the Eliassen–Kuo diagnostic equation (see appendix) governing the secondary (divergent) circulation to determine the processes responsible for the axisymmetric component of the moisture inflow.

Since the Eliassen–Kuo equation is elliptic for the parameters determined from the initial conditions and remains elliptic throughout the simulations, this equa-

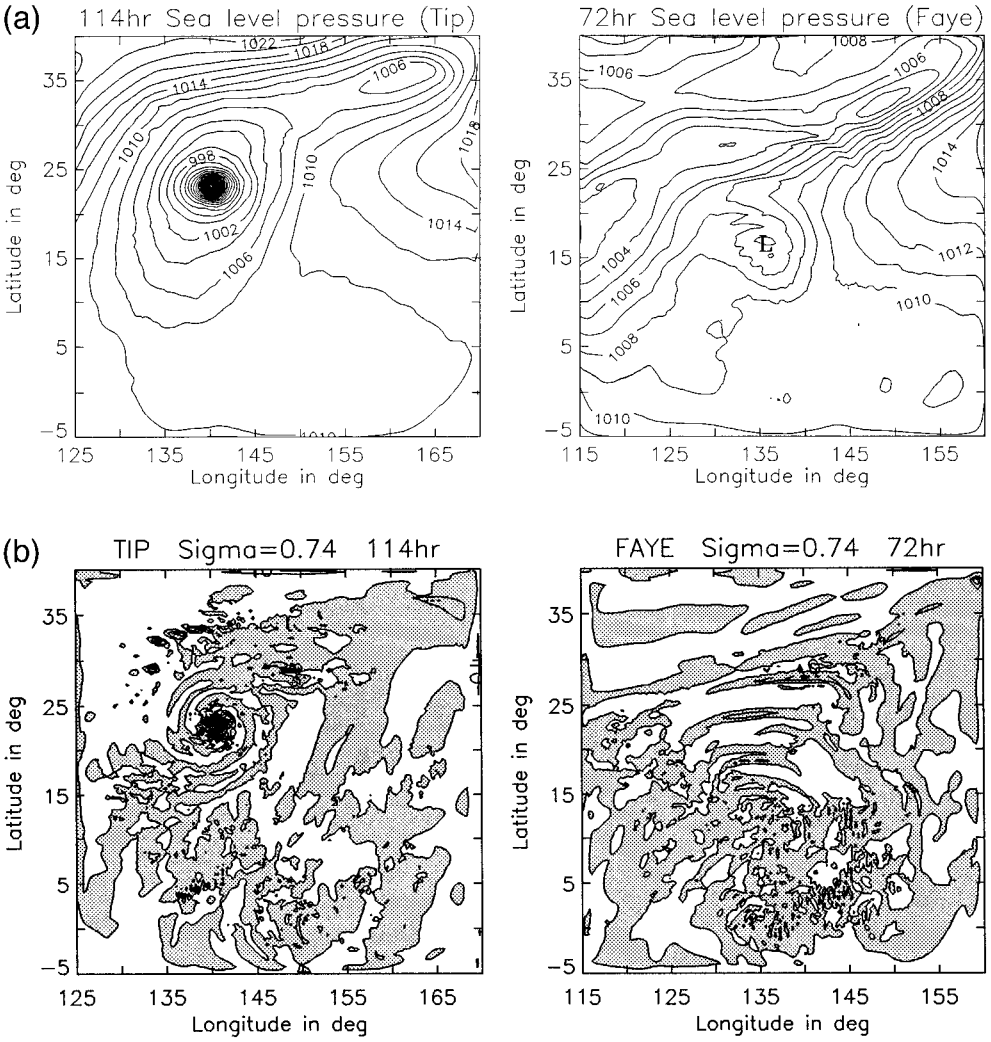

FIG. 6. (a) Surface pressure field (mb) at 114 h in the numerical simulation of Tip and at 72 h for Faye. (b) Horizontal distribution of vertical velocity ω at $\sigma = 0.74$, at 114 h for Tip and at 72 h for Faye in the numerical integrations. Contour interval is 1 Pa s^{-1} (shaded region represents upward motion).

tion dictates that a secondary circulation can exist only if it is forced by diabatic heating, friction, and/or eddy fluxes of heat and momentum across concentric circles centered on the vortex. Thus, although the eddy fluxes of specific humidity are outward in both Tip and Faye, the eddy fluxes of heat and momentum can drive an axially symmetric radial circulation that could transport moisture inward or outward depending on the spatial distributions of these fluxes. Before examining the different processes individually, we compare the radial flux of specific humidity in Tip and Faye accomplished by the axisymmetric component of the flow (as determined from the output of the model integrations) with that determined by solving the Eliassen–Kuo diagnostic equation with the forcing function consisting of the sum of all four processes at the end of 30 min of model simulation. Figure 9 reveals that both the model data and the solution of the Eliassen–Kuo equation give moisture flux by the axisymmetric component into Tip and out of Faye, increasing in magnitude with radius. The magnitude of the flux is, however, overestimated by the Eliassen–Kuo equation in the inner core.

We turn next to the processes responsible for the inward moisture flux in Tip and the outward flux in Faye accomplished by the axisymmetric secondary circulation. Since the Eliassen–Kuo equation is linear, the total solution for the secondary circulation induced by the sum of all processes is equal to the sum of the solutions for each of the different processes. We plot in Fig. 10 cross sections in the *r–p* plane of the components of the streamfunction, with arrows showing the direction, of the radial circulation induced by eddy fluxes of momentum and heat, friction and diabatic heating at the same time as in Figs. 8 and 9. The eddy-induced radial circulation in Tip (left-hand panel in Fig. 10c) is seen to be inward over a very large distance in the lower

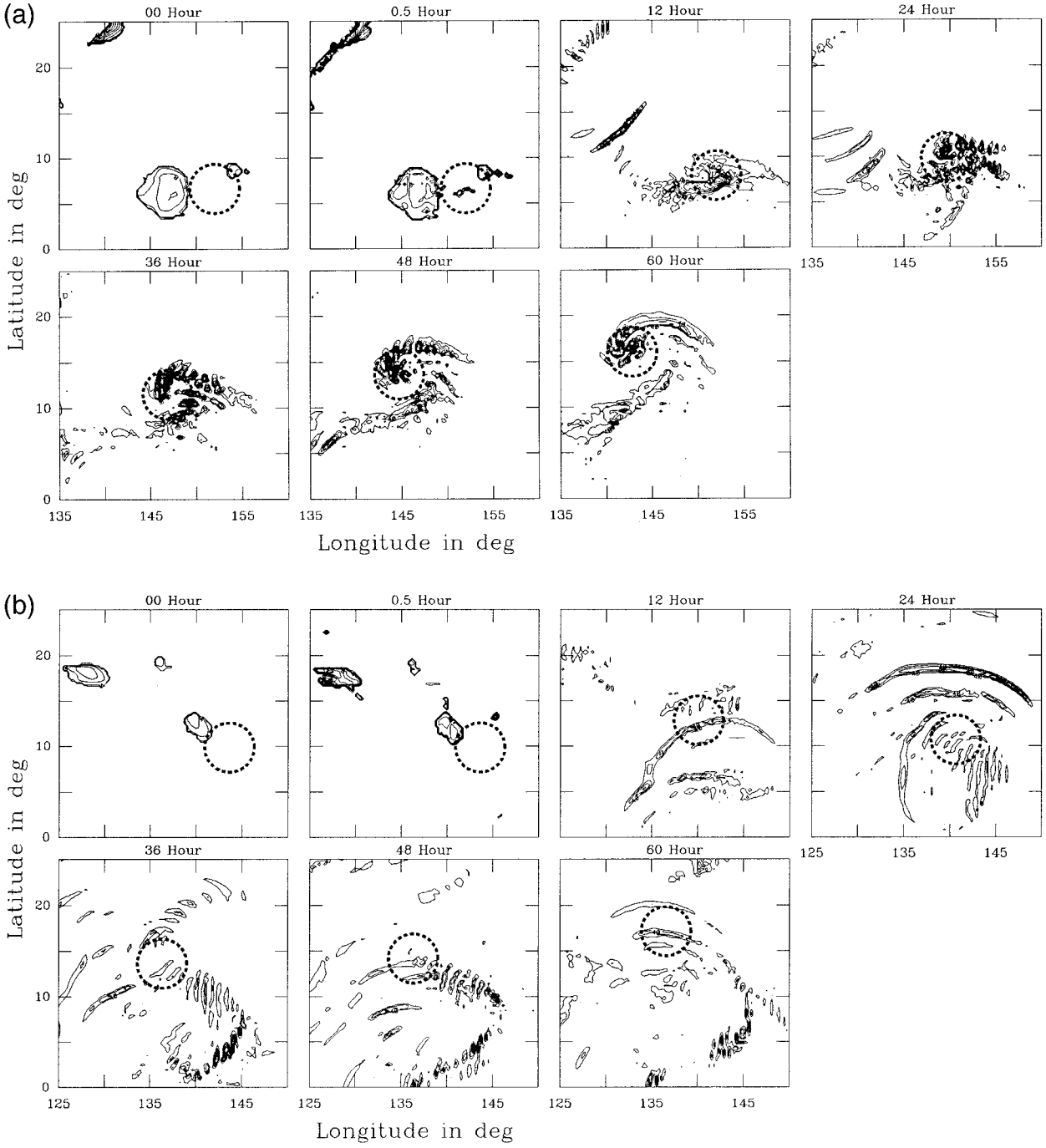

FIG. 7. (a) Horizontal distribution of latent heat release at $\sigma = 0.35$ at 0, 0.5, 12, 24, 36, 48, and 60 h of integration in the model simulation of Tip. Contour interval for 0 and 0.5 h is 2×10^{-5} K s^{-1} and 20×10^{-5} K s^{-1} for the others. (b) Same as (a) except for Faye.

troposphere, upward at small radii, and outward in the upper troposphere. In Faye (right-hand panel) it is in the opposite sense, namely, inward in the upper troposphere, downward at small radii, and outward over most of the lower troposphere. The friction-induced radial circulation (Fig. 10d) is shallow in both disturbances, with inward flow at the bottom and outward return flow immediately above it in the lower troposphere. The component of the radial circulation induced by diabatic heating (Fig. 10e) is directed inward in the lower troposphere only at radii larger than 300 km in both disturbances with a weak reverse circulation at small radii. The latter feature is a reflection of the fact that the primary centers of latent heat release in both

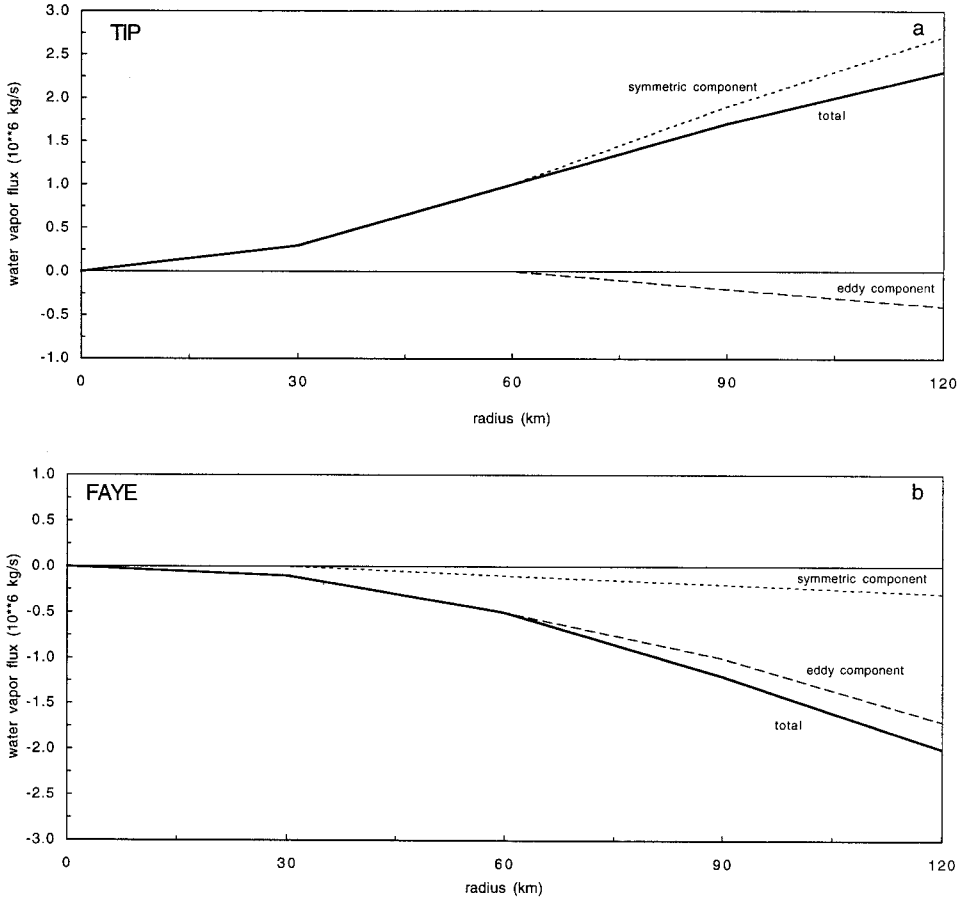

FIG. 8. Vertically integrated net moisture flux as a function of radius from the center of the disturbance for each simulation at 0.5 h of integration. Dotted line represents the azimuthal mean (symmetric) component, dashed line represents eddy component (departure from the mean), and the solid line the total of these two fluxes: (a) Tip and (b) Faye.

disturbances are significantly far removed from the vortex center. The resulting secondary circulations throughout most of the troposphere in Tip and Faye (Fig. 10f), dominated by the eddy-induced component at small radii in both disturbances and at all radii in Faye, are directed clockwise in the *r–p* plane in Tip and counterclockwise in Faye.

In Figs. 11a,b we show the contributions to the radial flux of specific humidity in the inner cores of Tip and Faye at 30 min by the eddy-, friction-, and heating-induced secondary circulations obtained from solutions of the Eliassen–Kuo diagnostic equation. The heavy solid curves (positive influx in Tip and negative in Faye, increasing in magnitude with radius) are the same as the solid curves labeled ''Eliassen–Kuo diagnostic'' in Fig. 9. The curves with the longer dashes represent the moisture fluxes accomplished by the eddy-induced radial circulations. In both disturbances this is the dominant contribution in the inner core (inward in Tip and outward in Faye). The curves with the shorter dashes and those with the dash–dot pattern represent the moisture fluxes accomplished by the friction- and heating-induced circulations, respectively. Friction induces a moisture inflow into both vortex centers, whereas the pattern of latent heat release is such as to induce a weak inward moisture inflow in Tip and an even weaker moisture outflow in Faye. Since the latent heat release does not appear in the vortex center of Tip before 30 min, and since it provides a small contribution at that time, we conclude that the initial organization and moisture supply is not due to the latent heat release. Rather, the latent heat release is the result of the inflow of moisture brought about by other processes, namely, the friction- and eddy-induced secondary radial circulation. The magnitude of the moisture flux induced by friction is smaller than that induced by the eddies and vanishes at radii smaller than 30 km in both Tip and Faye. The most dramatic difference between the two disturbances in regard to the moisture flux is that the component of this flux induced by the eddy fluxes of heat and momentum, which is the dominant one, is inward in Tip and outward in Faye. Moreover, there is a comparatively large water vapor outflow in Faye accomplished by the eddy flux $\overline{v_r' q'}$.

While the Kuo parameterization scheme in the model

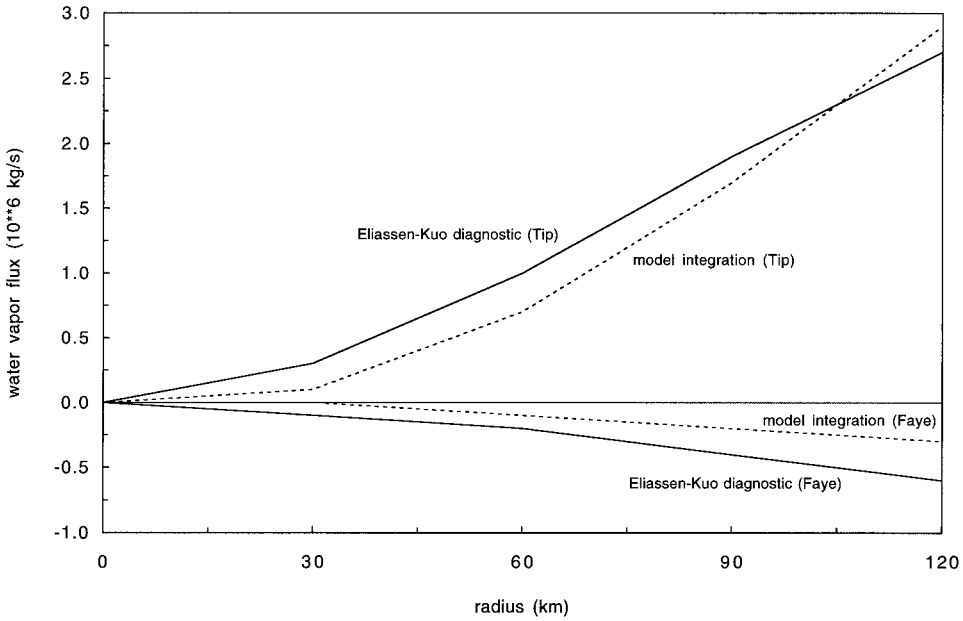

FIG. 9. Vertically integrated net moisture flux as a function of radius for Tip and Faye at 0.5 h of integration. Dashed line represents the axisymmetric component from the model integration and the solid line represents the Eliassen–Kuo solution forced by eddy fluxes of momentum and heat, friction, and latent heat.

gives cumulus convection wherever there is mass convergence in the boundary layer and moisture convergence in the air column, moist air in the real atmosphere must be raised to the lifting condensation level in order to support such convection. In order to determine the efficacy of the eddy-induced radial circulation in accomplishing this in the real atmosphere, we calculated the magnitude of the azimuthal mean vertical velocity in the vortex core induced by the eddy fluxes at the initial time and found it to be 0.22 cm s^{-1}. With the lifting condensation level ranging from approximately 85 to 160 m in Tip, it would require from 11 to 20 h for an air parcel at the surface to reach this level at these rates. Actually, since tropical disturbances are not axisymmetric, the local gridpoint values of the vertical motion are more than five times larger than the azimuthal mean, implying that, with the magnitude of the eddy flux forcing found in Tip, moist air parcels would reach the lifting condensation level in a matter of 2–4 h.

The foregoing results suggest that the secondary radial circulation induced by the eddy fluxes of heat and momentum can serve either as a catalyst for typhoon formation or as a mechanism for inhibiting the development of an incipient tropical disturbance, depending on the direction of the moisture transport (into or out of the vortex core). In the early stage of the life cycle of a typhoon, the surface winds are not strong enough to provide large amounts of local evaporation or to induce sufficiently large transports of moisture into the vortex core via frictional inflow in the Ekman layer to set off the convection and latent heat release required for self-sustained development. With the eddy flux of moisture $\overline{v_r' q'}$ of the wrong sign, the eddy-induced secondary circulation is the only remaining process available to concentrate the additional moisture required to trigger deep convection and latent heat release in the vortex core. Once a sufficiently well-organized center of deep convection is established in the core, the resulting latent heat release becomes the largest single forcing function driving the radial circulation, rapidly swamping the effect of the eddy flux forcing. Through the action of the Coriolis force, the surface circulation, and with it the Ekman pumping, intensifies. Increased evaporation associated with the stronger surface winds and increased moisture flux convergence associated with the stronger Ekman transport work together to maintain the moisture supply required for the subsequent explosive growth.

In connection with the latter scenario, it is of interest to see how the vertical velocity pattern develops with time during the first 24 h of the numerical simulation of Tip and to compare this with the early evolution in the simulation of Faye. In Fig. 12 we present the azimuthal mean vertical velocity distributions at the initial time and at 12 and 24 h of integration for both cases. It is significant that Tip develops vigorous (diabatically driven) upward motion concentrated near the vortex center, following the initial stage of eddy-induced upward motion, whereas Faye develops much weaker and more broadly distributed upward motion following the initial stage of broad-scale eddy-induced downward motion. By acting in the same direction as Ekman pumping, and with greater magnitude, the eddy-induced circulation in Tip clearly served as a catalyst for the devel-

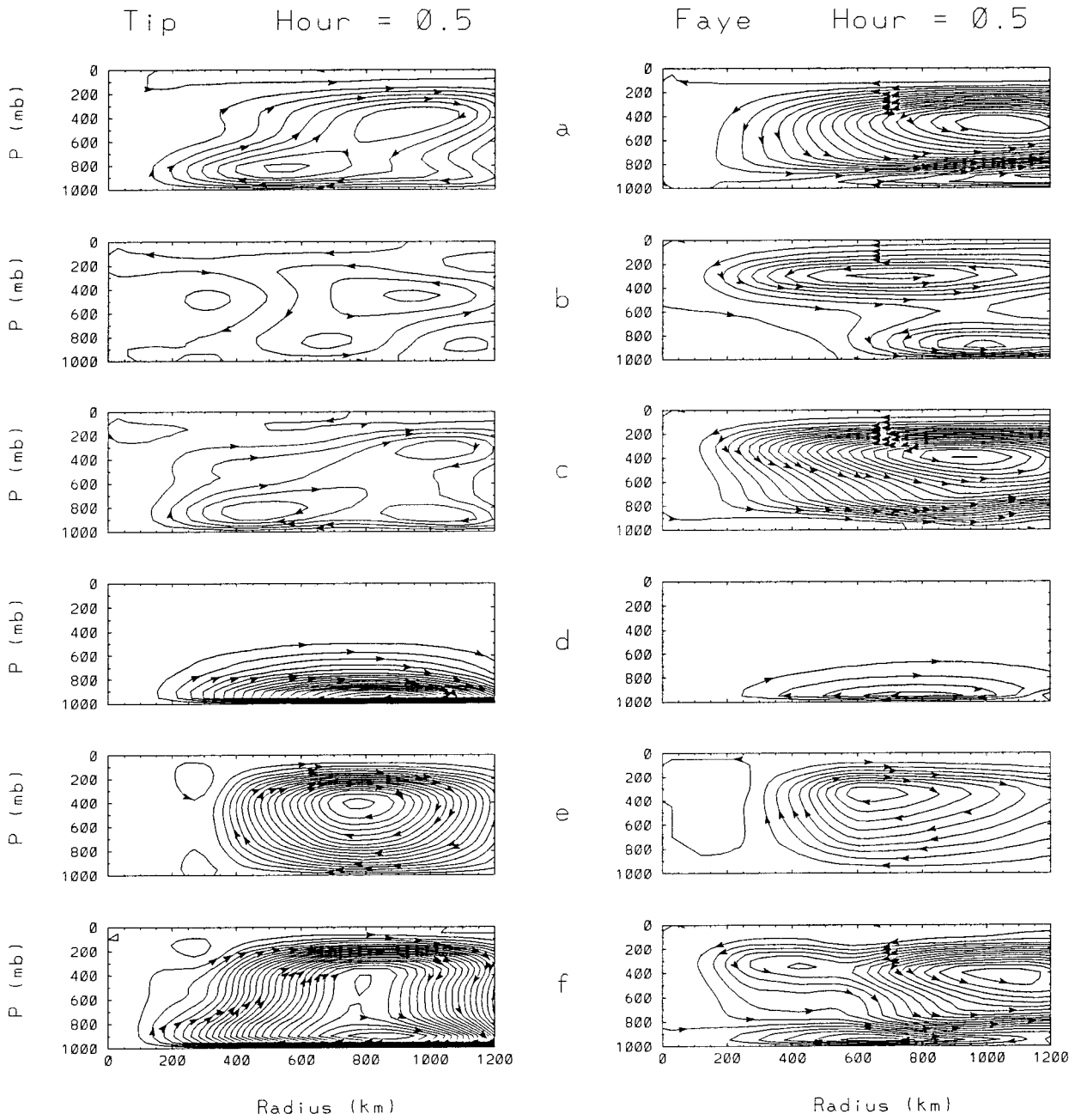

FIG. 10. Solutions of the Eliassen–Kuo diagnostic equation for the secondary circulation at 0.5 h of integration. The radial cross sections show the streamfunction forced by (a) the eddy fluxes of momentum, (b) the eddy fluxes of heat, (c) the sum of the eddy fluxes of momentum and heat, (d) the surface friction, (e) the latent heat of condensation, and (f) the total of all four of these processes at 0.5 h for each numerical simulation. Contour interval is 2×10^8 N s^{-1}.

opment of the diabatically driven circulation and the consequent formation of Tip into a typhoon. By acting in the opposite direction to Ekman pumping, again with greater magnitude, the eddy-induced circulation in Faye clearly added to the outward moisture flux by $\overline{v_r' q'}$ to inhibit the intensification of this disturbance into a typhoon.

Owing to the important catalytic effect of the large-scale eddy fluxes in Tip and Faye, it seems appropriate to investigate the distributions of the eddy fluxes of heat and momentum to see how they are organized to bring about the observed results. In Fig. 13 we show cross sections in the *r–p* plane of the radial eddy fluxes of heat and angular momentum calculated from the ECMWF FGGE data at the starting times for both numerical simulations (1200 UTC 7 Oct 1979 for Tip and

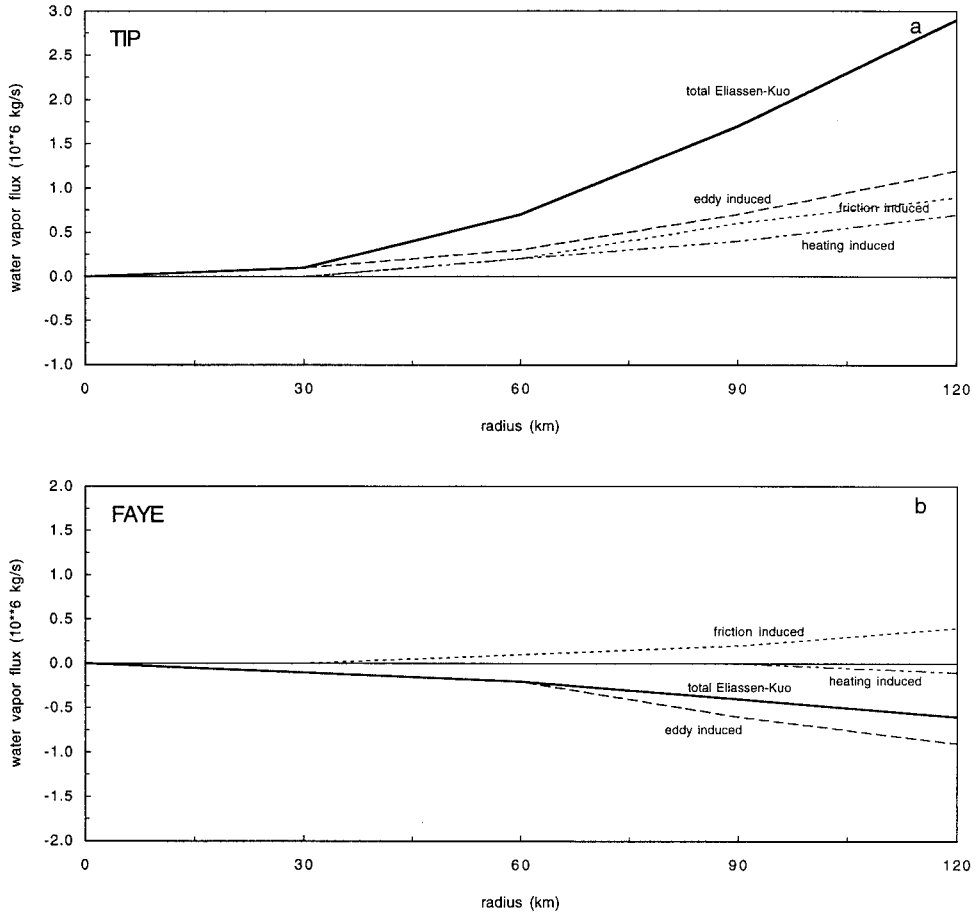

FIG. 11. Vertically integrated net moisture flux as a function of radius at 0.5 h obtained from the solution of the Eliassen–Kuo diagnostic equation. The dashed curve represents the moisture flux by the eddy-induced radial circulation, the dotted curve represents the moisture flux by the friction-induced radial circulation, the dot–dashed curve represents the moisture flux by the heating induced radial circulation. The solid curve is the sum of all the three processes: (a) Tip and (b) Faye.

0000 UTC 3 Jul 1979 for Faye). The temperature values required for the heat flux calculations were obtained from the geopotentials using the hydrostatic approximation with a virtual temperature correction. Calculations at the end of the first 30 min of integration (not shown) reveal that there is not much change in the distribution of these fluxes during the early stages of the numerical integration. While the heat flux patterns (Fig. 13b, with Tip on the left and Faye on the right) reveal differences between the two disturbances, the most striking difference is between the two angular momentum flux distributions (Fig. 13a). In particular, at large radii in the upper troposphere there is a well-organized influx of angular momentum in Tip and a well-organized outflux of angular momentum in Faye. Figure 14 shows that these fluxes were maintained for at least 24 h prior to the starting time for our simulations. The magnitude and distribution of the upper-tropospheric influx of angular momentum in the case of Tip is about the same as that shown by Pfeffer and Challa (1982) in the D1 case of McBride (1981b), which represents a composite of prehurricane cloud clusters.

It is instructive to look, too, at the upper-level wind patterns that bring about the momentum flux differences between the two cases. Figure 15 shows the wind vectors at 200 mb in both Tip and Faye at the time we started our integrations. We see that the flow around Tip is oriented such that, in the northeast quadrant of the circle (radius 1200 km), which is centered on the surface low, there is an inward transport of cyclonic angular momentum, and in the southwest quadrant there is an outward transport of anticyclonic angular momentum. The net effect of these two transports is an eddy influx of cyclonic angular momentum into the region at this elevation. In the case of Faye, the 200-mb wind vectors are oriented such that there is a strong transport of anticyclonic angular momentum into the region to the east and southeast of the storm center, and cyclonic angular momentum out of the region to the west of the center. The total outflow of cyclonic momentum in these two

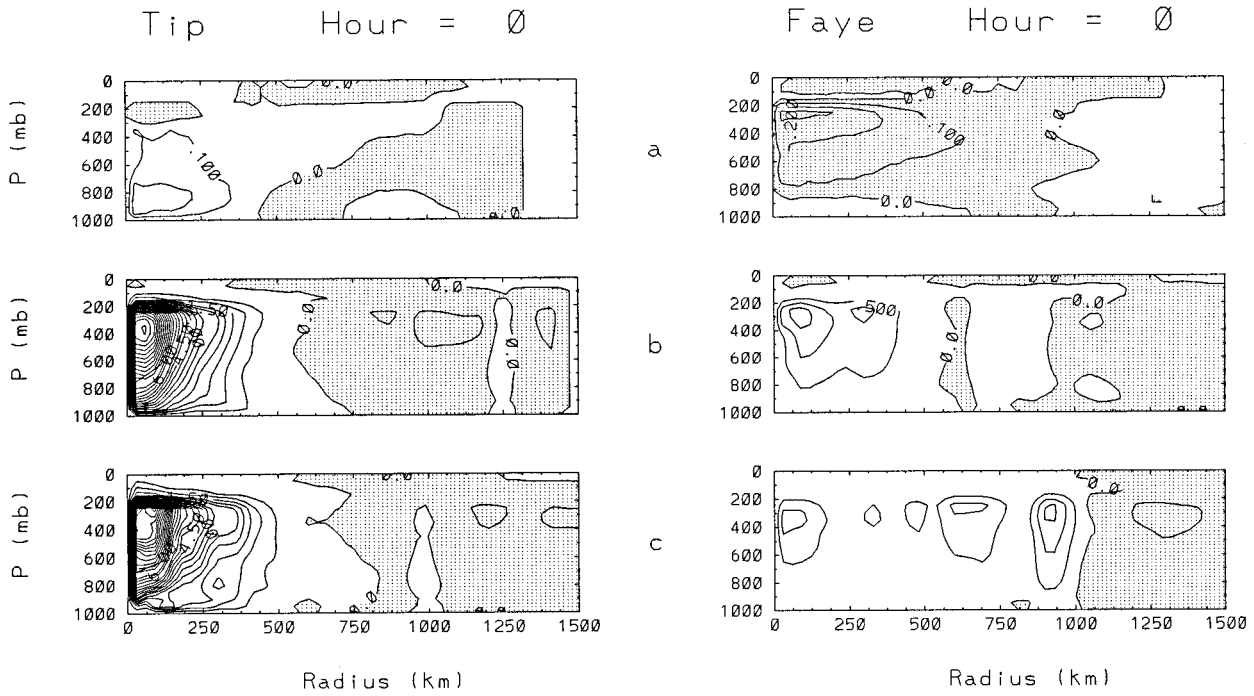

FIG. 12. Radial cross sections of the azimuthal mean vertical velocity $\overline{\omega}$ at 12-h intervals during the first 24 h of each numerical simulation starting with the initialized data (a) 0 h, (b) 12 h, (c) 24 h for Tip (left) and Faye (right). Contour interval for (a) 1×10^{-2} Pa s^{-1} and for (b) and (c) 5×10^{-2} Pa s^{-1}. Shaded regions represent downward motion (positive ω).

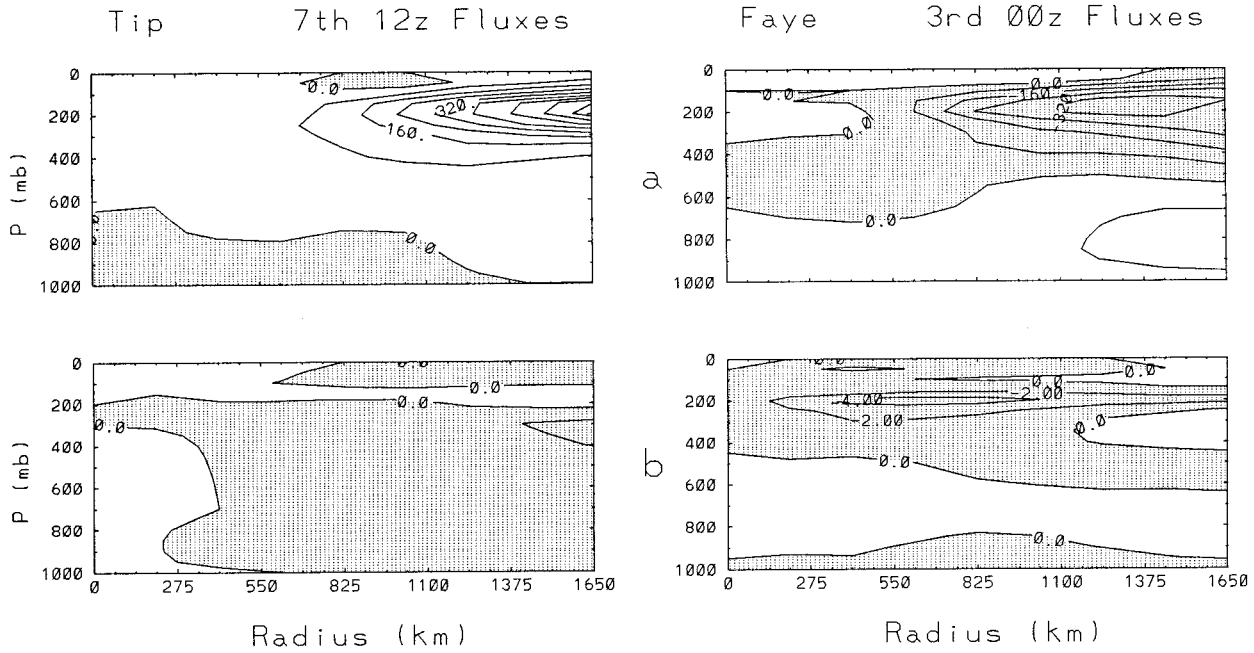

FIG. 13. Radial cross sections of the inward eddy fluxes of angular momentum $r\overline{v'_\theta v'_r}$ and heat $\overline{v'_r T'}$ per unit mass calculated from the ECMWF FGGE data for Tip 1200 UTC 7 October 1979 (left) and for Faye on 0000 UTC 3 July 1979 (right); (a) is eddy momentum flux, (b) is eddy heat flux. Here v_θ and v_r are the tangential and radial velocity components directed counterclockwise and inward, respectively, and r is radius. Contour interval is 80° lat m^2 s^{-2} for momentum and 2 K m s^{-1} for heat flux. Shaded region represents outward flux.

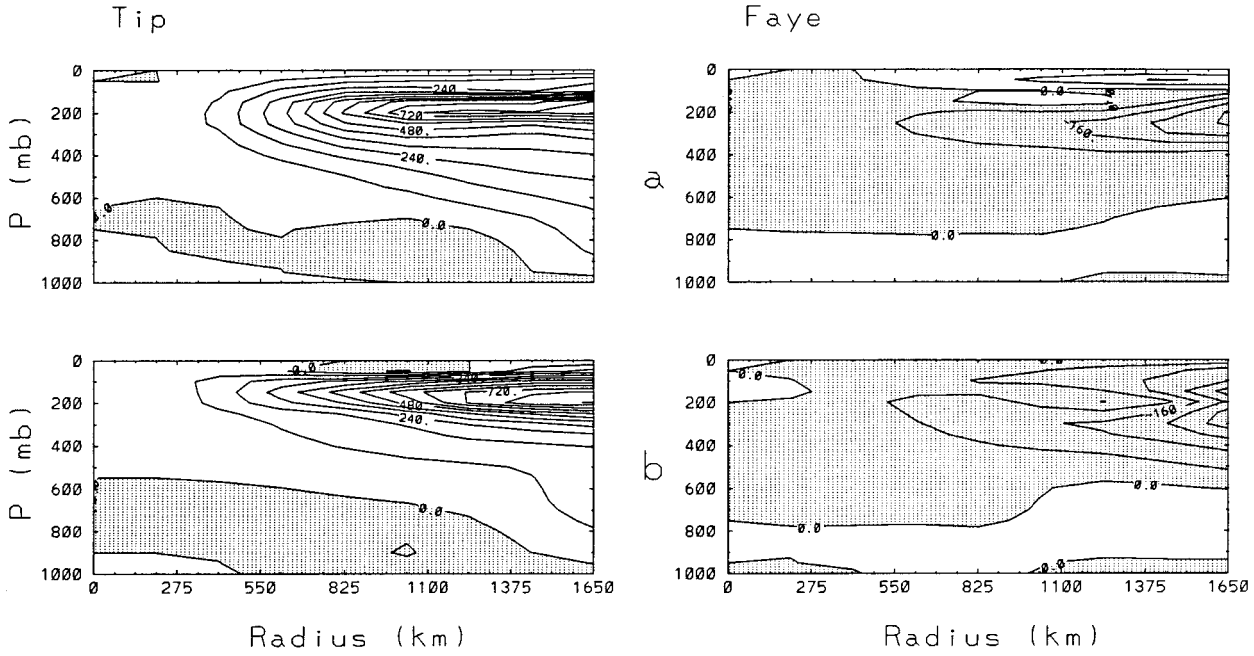

FIG. 14. Radial cross sections of the inward eddy fluxes of angular momentum $\overline{rv'_\theta v'_r}$ for Tip (left) and Faye (right) calculated from the ECMWF FGGE data (a) at t_0 minus 24 h and (b) at t_0 minus 12 h, where t_0 is the starting time for each numerical simulation. Contour interval is 80° lat m^2 s^{-2}. Shaded region represents outward flux.

locations exceeds the inflow across other sections of the circle, leading to a net outflow of angular momentum from the region. As shown in Fig. 13a, the eddy influx of angular momentum in Tip and outflux in Faye decrease in magnitude with decreasing radius and height. According to the Eliassen–Kuo equation (see appendix), the eddy momentum forcing function is proportional to the second derivative of the angular momentum flux with respect to radius and height, and its sign is such as to induce upper-level outflow and lower-level inflow in the case of Tip and the reverse in Faye, as shown in Fig. 10.

Among the other conditions often cited as requirements for the development of a tropical depression into a typhoon are that the 850–200-mb background wind shear be less than 12.5 m s^{-1} (Zehr 1992) (i.e, it should average less than 1.9 m s^{-1} per 100 mb) and that the sea surface temperature be greater than 26°C. The use

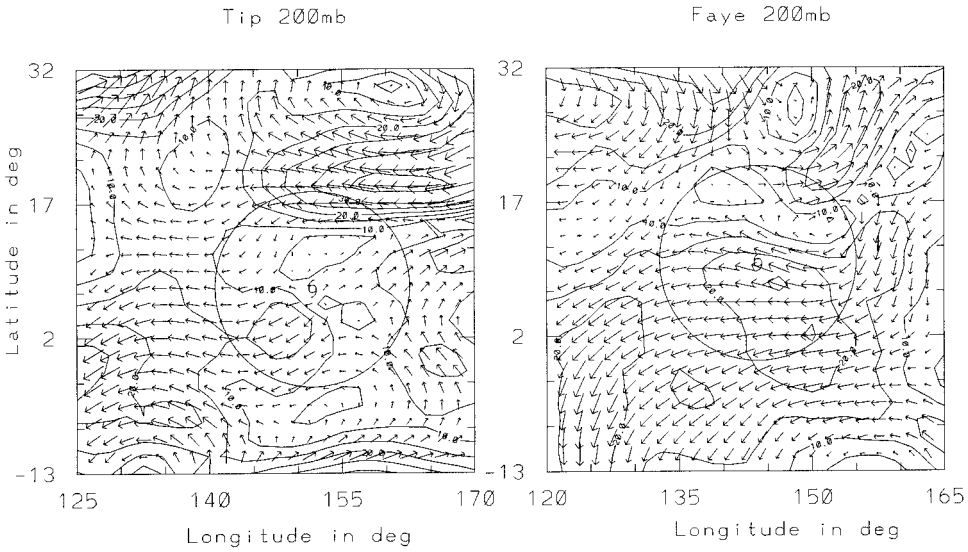

FIG. 15. Wind vectors and isotach distributions at 200 mb at 1200 UTC 7 October 1979 for Tip (left) and at 0000 UTC 3 July 1979 for Faye (right).

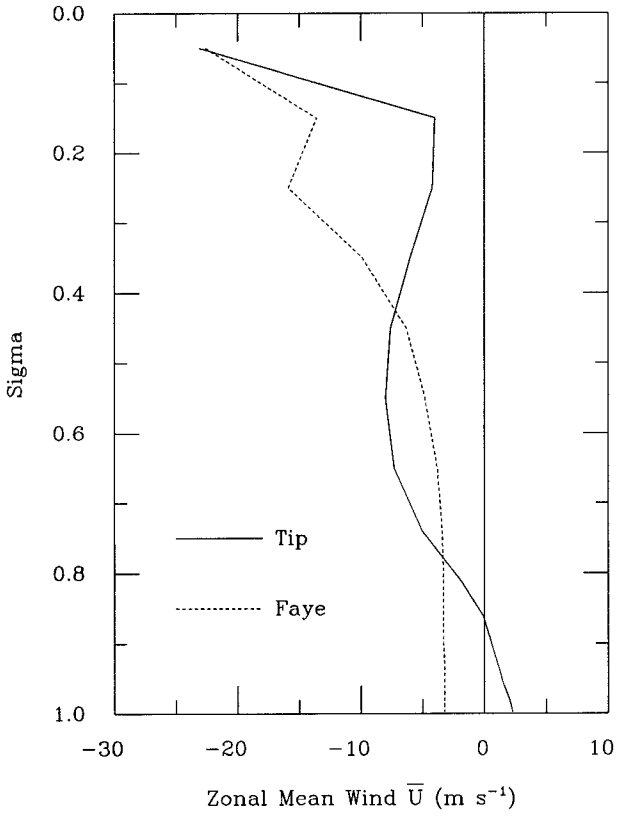

FIG. 16. The zonal wind averaged over a 600-km square centered on each disturbance at their initial time as a function of height (sigma).

of only two levels in assessing the vertical wind shear is necessitated in observational studies by the fact that cloud drift winds at these elevations are generally the only wind observations available in regions of typhoon formation. In the present study we do not have the same restrictions. The question naturally arises whether the differences in background wind shear and sea surface temperature between Tip and Faye can be considered important contributing factors to the difference in their evolutions.

The zonal wind profiles, averaged over a 600-km square centered on each disturbance at its respective initial time, are shown in Fig. 16. These profiles reveal that the wind shear between 850 and 200 mb is far from uniform with height. Tip had a significant easterly wind shear of 7.9 m s^{-1} (or about 2.6 m s^{-1} per 100 mb) between 850 and 550 mb and a westerly shear of 3.8 m s^{-1} between 550 and 250 mb (about 1.3 m s^{-1} per 100 mb). Owing to the reversal from easterly to westerly, the average wind shear between 850 and 250 mb appears deceptively small. Faye had a very weak wind shear between 850 and 550 mb and a large easterly shear of 11.1 m s^{-1} between 550 and 250 mb.

Elsberry and Jeffries (1996) found that large wind shears implied by NOGAPS analyses in the case of two developing tropical disturbances were overstated because the analyses did not capture the mesoscale features of the disturbance outflow layer. When they accounted for the disturbance outflow, they found much smaller wind shears that they attributed to the opposing or deflecting effects of the storm outflow (also concentrated in a shallow layer in the upper troposphere). The ECMWF global model analyses also do not capture mesoscale features of tropical disturbance outflow layers. The actual upper-layer wind shear associated with Faye could, therefore, have been smaller than is depicted in the ECMWF analyses. Nevertheless, even on the basis of the comparison shown in Fig. 16, it would be difficult to make the case that wind shear was a critical factor allowing the development of Tip and resulting in the nondevelopment of Faye.

While Tip and Faye are both located initially over water with sea surface temperatures greater than 29°C, fully 3°C greater than the threshold value required for typhoon formation, the SST distributions differ in that Tip has available a larger pool of very high temperature water through which to travel. In order to eliminate the differences in SST as a factor in the different evolutions of Tip and Faye, we repeated the numerical simulation of Faye using the same SST distribution that was used for the simulation of Tip. The resulting pressure drop was only 1–2 mb greater than that in the original run. We conclude, therefore, that the difference between the evolution of Faye and Tip was not related to SST differences.

6. Conclusions

We have extended our work on the role of eddy fluxes of momentum and heat in hurricane formation by simulating a developing and a nondeveloping tropical disturbance (Tip and Faye, respectively) from early stages in their life cycles and analyzing the differences in eddy flux distributions at the start of each simulation. We have also calculated the radial circulations and moisture influxes induced by these eddy fluxes, as well as by diabatic heating and friction. Our choice of diagnostics in terms of the axisymmetric circulation and departures from axisymmetry is based largely on the fact that the axisymmetric component of the circulation in fully developed typhoons is the dominant one, so it is instructive to investigate the role of the departures in initiating or suppressing the development of this circulation. The Eliassen–Kuo diagnostic equation provides a direct measure of the forcing of the ''in, up, and out'' component of the axisymmetric circulation that dominates the development of hurricanes and typhoons. While the diagnostics of hurricane development from the point of view of PV thinking provides another perspective, we are comfortable with the approach used in this study, which provides a clear link between the different scales of interaction that characterize the formation of hurricanes and typhoons.

As in our earlier studies with composite datasets, we

find that, in the formative stage, the developing disturbance (in this case Typhoon Tip) displays a large-scale pattern of eddy fluxes of momentum with a maximum around 200 mb at a distance of more than 1000 km from the center of lowest pressure, decreasing rapidly with decreasing radius and height. Such a flux distribution serves as a source that induces a secondary radial circulation with outflow in the upper troposphere and inflow in the lower troposphere over a broad stretch of warm ocean, thereby drawing moisture into the region, organizing the convection and providing lifting necessary to set off conditional instability. In Tip, this pattern was persistent for at least 24 h prior to the time we started our numerical simulation. While the eddy fluxes of heat in Tip contributed to a secondary circulation in the same direction, their contribution in this case was much smaller than that of the momentum fluxes. Moreover, the contributions of heating and friction were smaller than those of the eddy fluxes, particularly in the inner core of Tip.

Whereas the nondeveloping tropical disturbances in the composite datasets that we used in the past showed no well-organized eddy flux distributions, the eddy flux of momentum in the nondeveloping disturbance, Faye, was organized such that it was outward at 200 mb, decreasing in magnitude rapidly with decreasing radius and height from a maximum located more than 1000 km from the center of lowest pressure. This pattern, which was persistent for at least 24 h prior to the time we started our numerical simulation, induced a secondary circulation with inward motion in the upper troposphere and outward motion in the lower troposphere. By transporting water vapor away from the disturbance, this circulation helped to suppress deep convection, thereby preventing the development of Faye into a typhoon. An even larger outward flux of water vapor was accomplished by the processes $\overline{v_r' q'}$.

The results of this study provide additional evidence in support of the hypothesis that eddy fluxes of momentum and heat associated with synoptic-scale waves in the environment of an incipient tropical disturbance serve as a catalyst for hurricane and typhoon formation or as a means of suppression of intensification, depending on the distribution of the fluxes.

Acknowledgments. This research was supported by National Science Foundation Grant ATM-9310119 and partially from the Naval Research Laboratory Basic Research Program PE601153N. We would like to express our gratitude to Dr. R. V. Madala and K. Seshegyi for helpful discussions during this research and to Dr. C. Long for his help in computing. We would like to express our sincere thanks also to Scott Applequist, Mike Kirby, and Kevin Convery for their help in the graphics preparation. Computer time for the numerical integrations was furnished by the National Center for Atmospheric Research (NCAR), which is supported by the National Science Foundation. We wish to express our sincere appreciation to Mr. Ken Hansen of NCAR for his assistance in using the CRAY Y-MP 8/864 and J916 16/256. The first author would like to express his gratitude to Dr. D. Loper, director of the Geophysical Fluid Dynamics Institute, and Dr. A. Krothapalli, chairman, Department of Mechanical Engineering, for their support. Finally, we are grateful to the reviewers whose insightful comments forced us to do additional calculations, the results of which greatly strengthened this paper.

APPENDIX

The Radial Circulation Equation

The equation governing the radial circulation of a balanced vortex may be written in cylindrical coordinates (Sundqvist 1970; Pfeffer and Challa 1992), as follows:

$$A\frac{\partial^2\psi}{\partial p^2} + 2B\frac{\partial^2\psi}{\partial r\partial p} + C\frac{\partial^2\psi}{\partial r^2} - \frac{4B}{r}\frac{\partial\psi}{\partial p} - \left(\frac{1-\kappa}{p}B + \frac{C}{r}\right)\frac{\partial\psi}{\partial r}$$
$$= \frac{Rr}{p}\frac{\partial}{\partial r}\left(\frac{\overline{Q}}{c_p} - \frac{1}{r}\frac{\partial r\overline{v_r' T'}}{\partial r}\right)$$
$$+ r\frac{\partial}{\partial p}\left[\left(f + \frac{2\overline{v_\theta}}{r}\right)\left(\overline{F} - \frac{1}{r^2}\frac{\partial r^2\overline{v_\theta' v_r'}}{\partial r}\right)\right] \qquad \text{(A1)}$$

where

$$A = \left(f + \frac{2\overline{v_\theta}}{r}\right)\left(f + \frac{\partial\overline{v_\theta}}{\partial r} + \frac{\overline{v_\theta}}{r}\right)$$

dynamic stability parameter

$$B = -\left(f + \frac{2\overline{v_\theta}}{r}\right)\frac{\partial\overline{v_\theta}}{\partial p} = \frac{\alpha}{\theta}\frac{\partial\overline{\theta}}{\partial r}$$

baroclinic stability parameter

$$C = \frac{\alpha}{\theta}\frac{\partial\overline{\theta}}{\partial p}$$

static stability parameter.

Here, r is radius, p pressure, T temperature, θ potential temperature, α specific volume; v_θ and v_r are the tangential (positive counterclockwise) and radial (positive outward) components of the wind velocity, ψ is the Stokes streamfunction (given by $\overline{v}_r = (1/r)(\partial\psi/\partial p)$, and $\overline{\omega} = -(1/r)\partial\psi/\partial r$, where $\omega \equiv dp/dt$ and t is time); Q is the diabatic heating rate per unit mass, F the azimuthal component of the boundary layer friction force per unit mass, f the Coriolis parameter, R the gas constant for dry air, c_p the specific heat capacity of the air at constant pressure, $\kappa = R/c_p$, the overbar represents an azimuthal mean, and the primes designate departures from this mean. In Eq. (A1) we have neglected the vertical eddy fluxes of momentum and heat.

REFERENCES

Black, P. G., and R. A. Anthes, 1971: On the asymmetric structure of the tropical cyclone outflow layer. *J. Atmos. Sci.,* **28,** 1348–1366.

Bourke, W., and J. L. McGregor, 1983: A nonlinear vertical mode initialization scheme for a limited area prediction model. *Mon. Wea. Rev.,* **111,** 2285–2297.

Businger, J. A., J. C. Wyngaard, Y. Izumi, and E. F. Bradley, 1971: Flux-profile relationship in the atmospheric surface layer. *J. Atmos. Sci.,* **28,** 181–189.

Challa, M., and R. L. Pfeffer, 1980: Effects of eddy fluxes of angular momentum on the model hurricane development. *J. Atmos. Sci.,* **37,** 1603–1618.

——, and ——, 1984: The effect of cumulus momentum mixing on the development of a symmetric model hurricane. *J. Atmos. Sci.,* **41,** 1312–1319.

——, and ——, 1990: Formation of Atlantic hurricanes from cloud clusters and depressions. *J. Atmos. Sci.,* **47,** 909–927.

——, and ——, 1992: Some aspects of hurricane formation. *Trends Atmos. Sci.,* **1,** 15–25.

Chang, S. W., and T. R. Holt, 1994: Impact of assimilating SSM/I rainfall rates on numerical prediction of winter cyclones. *Mon. Wea. Rev.,* **122,** 151–164.

——, ——, and K. Sashegyi, 1996: A numerical study of the ERICA IOP4 marine cyclone. *Mon. Wea. Rev.,* **124,** 27–46.

Charney, J. G., and A. Eliassen, 1964: On the growth of the hurricane depression. *J. Atmos. Sci.,* **21,** 68–75.

Davidson, N. E., G. J. Holland, J. L. McBride, and T. D. Keenan, 1990: On the formation of AMEX Tropical Cyclones Irma and Jason. *Mon. Wea. Rev.,* **118,** 1981–2000.

Dell'osso, L., and L. Bengtsson, 1985: Prediction of a typhoon using a fine-mesh NWP model. *Tellus,* **37A,** 97–105.

DeMaria, M., J.-J. Baik, and J. Kaplan, 1993: Upper-level eddy angular momentum fluxes and tropical cyclone intensity change. *J. Atmos. Sci.,* **50,** 1133–1147.

Eliassen, A., 1952: Slow thermally or frictionally controlled meridional circulations in a circular vortex. *Atmosphys. Norv.,* **5,** 19–60.

Elsberry, R. L., and R. A. Jeffries, 1996: Vertical wind shear influences on tropical cyclone formation and intensification during TCM-92 and TCM-93. *Mon. Wea. Rev.,* **124,** 1374–1387.

Emanuel, K., 1986: An air–sea interaction theory for tropical cyclones. Part I: Steady state maintenance. *J. Atmos. Sci.,* **43,** 585–604.

——, 1989: The finite-amplitude nature of tropical cyclogenesis. *J. Atmos. Sci.,* **46,** 3431–3456.

Frank, W. M., 1977: The structure and energies of the tropical cyclone: II. Dynamics and energetics. *Mon. Wea. Rev.,* **105,** 1136–1152.

Gerber, H. S., S. W. Chang, and T. Holt, 1989: Evolution of a marine boundary layer jet. *J. Atmos. Sci.,* **46,** 1312–1326.

Holt, T. R., S. W. Chang, and S. Raman, 1990: A numerical study of the coastal cyclogenesis in GALE IOP2: Sensitivity to PBL parameterization. *Mon. Wea. Rev.,* **118,** 234–257.

Kolmogorov, A. N., 1942: The equation of turbulent motion in an incompressible fluid. *Izv. Akad. Nauk USSR Ser. Fiz.,* **6,** 56–58.

Krishnamurti, T. N., S. Low-Nam, and R. Pasch, 1983: Cumulus parameterization and rainfall rates II. *Mon. Wea. Rev.,* **111,** 815–828.

Kuo, H. L., 1956: Forced and free meridional circulations in the atmosphere. *J. Meteor.,* **13,** 561–568.

——, 1974: Further studies of the parameterization of the influence of cumulus convection on large-scale flow. *J. Atmos. Sci.,* **31,** 1232–1240.

Madala, R. V., 1981: Efficient time integration schemes for atmospheric and ocean models. *Finite Difference Techniques for Vectorized Fluid Dynamics Calculations,* David L. Book, Ed., Springer-Verlag, 56–70.

——, and S. W. Chang, 1979: A vectorized three-dimensional operational tropical cyclone model. *Proc. Scientific Computer Informational Exchange Meeting,* Livermore, CA, Office of Naval Research, 47–52.

——, ——, U. C. Mohanty, S. C. Madan, R. K. Paliwal, V. B. Sarin, T. Holt, and S. Raman, 1987: Description of Naval Research Laboratory limited area dynamical weather prediction model. NRL Tech. Rep. 5992, 131 pp. [NTIS A182780.]

McBride, J., 1981a: Observational analysis of tropical cyclone formation. Part I: Basic description of data sets. *J. Atmos. Sci.,* **38,** 1117–1131.

——, 1981b: Observational analysis of tropical cyclone formation. Part III: Budget analysis. *J. Atmos. Sci.,* **38,** 1152–1166.

——, and R. Zehr, 1981: Observational analysis of tropical cyclone formation. Part II: Comparison of non-developing vs. developing systems. *J. Atmos. Sci.,* **38,** 1132–1151.

Molinari, J., and D. Vollaro, 1989: External influences on hurricane intensity. Part I: Outflow layer eddy angular momentum fluxes. *J. Atmos. Sci.,* **46,** 1093–1105.

——, and ——, 1990: External influences on hurricane intensity. Part II: Vertical structure and response of the hurricane vortex. *J. Atmos. Sci.,* **47,** 1902–1918.

Monin, A. S., and A. M. Yaglom, 1971: *Statistical Fluid Mechanics.* Vol. 1. The MIT Press, 769 pp.

Montgomery, M. T., and B. F. Farrell, 1993: Tropical cyclone formation. *J. Atmos. Sci.,* **50,** 285–310.

Ooyama, K., 1964: A dynamical model for the study of tropical cyclone development. *Geofis. Int.,* **4,** 187–198.

Palmen, E., and H. Riehl, 1957: Budget of angular momentum and energy in tropical cyclones. *J. Meteor.,* **14,** 150–159.

Pfeffer, R. L., 1956: A discussion of the balance of angular momentum in hurricanes. *Bull. Amer. Meteor. Soc.,* **37,** 234.

——, 1958: Concerning the mechanics of hurricanes. *J. Meteor.,* **15,** 113–120.

——, 1965: Dynamics of hurricane motion. *Geof. Int.,* **5,** 119–129.

——, and M. Challa, 1981: A numerical study of the role of eddy fluxes of momentum in the development of Atlantic hurricanes. *J. Atmos. Sci.,* **38,** 2393–2398.

——, and ——, 1982: Model development of Atlantic hurricanes from pre-hurricane cloud clusters, depressions and cyclones. *Intense Atmospheric Vortices,* L. Bengtsson and J. Lighthill, Eds., Springer-Verlag, 81–94.

——, and ——, 1992: The role of environmental asymmetries in Atlantic hurricane formation. *J. Atmos. Sci.,* **49,** 1051–1059.

——, and ——, 1993: Model hurricane formation in the presence of a basic state current. *Atmosfera,* **6,** 25–37.

Sashegyi, K. D., and R. V. Madala, 1993: Application of vertical-mode initialization to a limited-area model in flux form. *Mon. Wea. Rev.,* **121,** 207–220.

Shi, J.-J., S. Chang, and S. Raman, 1997: Interaction between Hurricane Florence (1988) and an upper-tropospheric westerly trough. *J. Atmos. Sci.,* **54,** 1231–1247.

Sundquist, H., 1970: Numerical simulation of the development of tropical cyclones with a ten-level model. Part 1. *Tellus,* **22,** 369–390.

Zehr, R. M., 1992: Tropical cyclogenesis in the western North Pacific. NOAA Tech. Rep. NESDIS 61, 181 pp. [Available from Department of Commerce, Washington, DC 20233.]